Res Chem Intermed (2013) 39:597–614
DOI 10.1007/s11164-012-0582-1

Synthesis of a novel betaine-type asphalt emulsifier and its investigation by online FTIR spectrophotometry

Chunlei Huai · Laishun Shi · Na Li

Received: 5 March 2012 / Accepted: 26 April 2012 / Published online: 17 May 2012

Abstract A novel betaine-type asphalt emulsifier, 3-(dodecyloxy)-2-hydroxypropan-*N*-carboxymethyl-*N*,*N*-dimethylammonium chloride, has been synthesized in a three-step reaction from lauryl alcohol, epichlorohydrin, dimethylamine, and chloroacetic acid. The optimum reaction conditions were obtained for synthesis of 2-(dodecyloxymethyl)oxirane in the first step. The yield reaches 75.7 % under the optimum conditions of reaction temperature 50 °C, reaction time 5 h, feedstock mole ratio of epichlorohydrin to lauryl alcohol 1.4, basicity 33.3 %. The structures of the three products were identified by FTIR. Synthesis of 2-(dodecyloxymethyl)oxirane in the first step was monitored by online FTIR, and an intermediate was detected. On the basis of the experimental data, a plausible reaction mechanism was proposed for the reaction. The critical micelle concentration (CMC) of the final product is low, 8.8×10^{-5} mol/L. The surface tension at the CMC is 21.2 mN/m. This product is an excellent emulsifier for asphalt. The prepared bituminous emulsion had high storage stability. The emulsifier is a rapid-set asphalt emulsifier.

Keywords Asphalt · Emulsifier · Betaine · Synthesis · Online FTIR

Introduction

Surfactants to emulsify water and asphalt are called asphalt emulsifiers. The prepared solution is called a bituminous emulsion. Compared with hot asphalt, use of a bituminous emulsion has the advantage of stronger adhesive power with mineral aggregate, lower energy consumption, and less pollution of the environment. Bituminous emulsions are widely used as pavement and building materials [1–3].

C. Huai · L. Shi (✉) · N. Li
School of Chemistry and Chemical Engineering, South Campus, Shandong University, Jinan 250061, People's Republic of China
e-mail: lshunsh@sdu.edu.cn

Depending on the nature of the electric charge on the molecule, asphalt emulsifiers are divided into anionic types, cationic types, zwitterionic types, and nonionic types. Anionic emulsifiers, for example long-chain sulfonate, alkali metal salts of an alkaline lignin, and carboxylic acid organic salts, were widely used in the early stage of research [4–6]. Cationic emulsifiers replaced anionic emulsifiers later because of their better emulsifying performance and excellent adhesive power with mineral aggregate [7, 8]. The main cationic asphalt emulsifiers are organic amines, quaternary ammonium salts, and imidazoline [9]. Peter Schilling studied the emulsifying compositions of fatty amine and/or polyamine, lignin, and nonionic surfactants. A preferred emulsifying composition can be produced by reacting combinations of fatty amine and/or polyamine, lignin, and nonionic surfactant with formaldehyde [10]. Gemini emulsifier is a kind of surfactant with more hydrophilic groups and lipophilic groups, and it has stronger emulsifying ability [11–13]. Shi et al. [14] studied the new Gemini cationic asphalt emulsifier bis[5-nonyl-2-((2′-hydroxy-3′-triethyl ammonium chloride)propyl-oxy-benzyl)]methane, which was synthesized by reaction of triethylamine, epichlorohydrin, and bis(2-hydroxy-5-nonyl phenyl)methane, prepared from nonylphenol and formaldehyde. In addition, combination of different asphalt emulsifiers can achieve the emulsifying ability desired. Graf et al. [15] studied a medium set cationic bituminous emulsion comprising asphalt, a cationic emulsifier and a nonionic water-soluble thickening agent.

Zwitterionic emulsifiers, which can be mainly divided into betaine types and amino acids, are another active research area of surfactants [16]. The hydrophilic groups in the molecular structures contain both acidic and alkaline groups and their charge properties depend on pH. The alkaline group of betaine emulsifier molecules is quaternary ammonium whereas the acidic groups are mainly carboxyl and sulfonic acid. A variety of research has been conducted on betaine emulsifiers [17–20]. They have good solubility, are less affected by pH than amino acids, and are not precipitated at the isoelectric point. They have excellent emulsifying properties and good compatibility with anionic, cationic, and nonionic surfactants [21, 22].

In previous work we studied different types of asphalt emulsifiers [14]. In this study, a new betaine-type asphalt emulsifier with better emulsifying properties was synthesized. The synthetic route to the emulsifier was optimized. The chemical structures were characterized by FTIR. An intermediate was detected by online FTIR analysis. A plausible reaction mechanism was proposed for the reaction.

Experimental

Materials

Lauryl alcohol was obtained from Sinopharm Chemical Reagent, Shanghai, China. Chloroacetic acid was purchased from Tianjin DaMao Chemical Reagent Factory, Tianjin, China. Epichlorohydrin and dimethylamine (33 %) were obtained from XiLong Chemical Reagent, Guangzhou, China. All these reagents were of analytical grade and used without further purification. The asphalt used was AH-90, which was

provided by Shengli Refinery of Qilu Petrochemical Company, Zibo, China. The mineral aggregate was of marble stone mixture of different size.

Synthesis of betaine-type asphalt emulsifier

Scheme 1 shows the synthetic route to the asphalt emulsifier.

2-(Dodecyloxymethyl)oxirane (a): Lauryl alcohol (18.6 g, 0.10 mol) was dissolved in 20.0 mL petroleum ether, then NaOH (5.0 g), tetrabutyl ammonium bromide (0.8 g), and 10.0 mL water were added. Epichlorohydrin (13.0 g, 0.14 mol) was then added dropwise and the mixture was stirred for 5 h at 50 °C in a water bath. The resulting precipitate was rinsed three times with petroleum ether and then the inorganic salt was removed. The final product was obtained by vacuum distillation.

1-(*N*,*N*-Dimethylamino)-3-(dodecyloxy)propan-2-ol (b): 33 % Dimethylamine aqueous solution (15.0 g, 0.11 mol) was added dropwise to 2-(dodecyloxymethyl)oxirane synthesized above and the mixture was stirred for 6 h at 65 °C in a water bath. The aqueous phase was removed by means of separatory funnel. The oil phase was processed by vacuum distillation to remove the solvent, then recrystallized from a mixture of ethyl acetate and petroleum ether. Product b was dried to a constant weight under vacuum. The yield of product b was 50.6 %, which was calculated from the weight obtained.

3-(Dodecyloxy)-2-hydroxypropan-*N*-carboxymethyl-*N*,*N*-dimethylammonium chloride (c): Chloroacetic acid (11.5 g, 0.12 mol) was added to 1-(*N*,*N*-dimethylamino)-3-(dodecyloxy)propan-2-ol (b) synthesized above and the mixture was stirred for 6 h at 65 °C in a water bath. The reaction solution was processed by vacuum distillation to remove the solvent and obtain the crude product. The crude

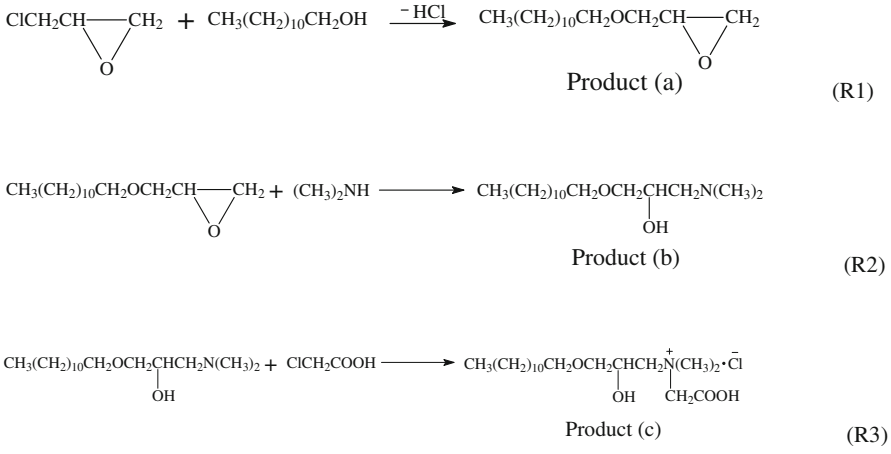

Scheme 1 Synthetic route to 3-(dodecyloxy)-2-hydroxypropan-*N*-carboxymethyl-*N*,*N*-dimethyl ammonium chloride

product was recrystallized from ethanol (33 %), and dried to constant weight under vacuum. The yield of product c was 96.7 %.

The yields (Y) of products a and c were obtained by the Mohr method. In reaction R1, chloride ion was produced. 5.0000 g aqueous phase sample was weighed into a conical flask, then approximately 50 mL distilled water and 0.1 mL of phenolphthalein indicator were added. The solution was titrated with 0.1 mol/L standard nitric acid solution until complete loss of color. Then 1 mL 5 % potassium chromate indicator was added and the solution was titrated with 0.1 mol/L standard silver nitrate solution. The endpoint of the titration was identified as the first appearance of the red–brown color of silver chromate. At the same time, a blank titration was performed.

$$Y = \frac{N \times (V - V_0) \times m'}{1000 \times m \times n} \times 100\%$$

where V is the volume of $AgNO_3$ standard solution consumed (mL), V_0 is the volume of $AgNO_3$ standard solution consumed in the blank test (mL), m' is the total mass of the aqueous phase sample (g), m is the mass of the aqueous phase sample to be titrated (g) N is the concentration of $AgNO_3$ standard solution (mol/L), and n is the number of moles of lauryl alcohol.

Surface tension and critical micelle concentration (CMC)

The surface tension of surfactant solutions decreases sharply with increasing concentration, then hardly changes when the concentration reaches the CMC. The surface tension of surfactant solutions was measured with a Krüss (Hamburg, Germany) Processor Tensiometer K12. The CMC and the surface tension at the CMC were determined from the breaking point of the curve of surface tension plotted against the logarithm of the concentration.

FTIR analysis

FTIR spectra were recorded in the wavenumber range 400 to 4,000 cm^{-1}, with averaging of 32 scans at a resolution of 4 cm^{-1}, on a Bruker Tensor-27 FTIR spectrophotometer.

UV–visible spectroscopic analysis

UV–visible spectroscopy was performed with a TU-1800PC UV–Vis spectrophotometer (Beijing Puxi Tongyong Instrument Company, Beijing, China). Complete spectra of 0.5200 g lauryl alcohol or product c in 50 mL ethanol solution were obtained in the range 200–1,000 nm.

Online FTIR analysis during synthesis of 2-(dodecyloxymethyl)oxirane

Online FTIR analysis was performed with a ReactIR 4000 spectrophotometer (Mettler–Toledo AutoChem, USA). FTIR spectra were recorded in the wavenumber

range 650 to 4,000 cm^{-1} at a resolution of 8 cm^{-1}. Lauryl alcohol (18.6 g, 0.10 mol) was dissolved in 20.0 mL petroleum ether. NaOH (5.0 g), tetrabutyl ammonium bromide (0.8 g), and 10.0 mL water were added. The solution was stirred and heated to 50 °C in a water bath. The detector of the online FTIR analysis system was immersed in the solution and the system then started to record the 3D spectra. Epichlorohydrin (13.0 g, 0.14 mol) was added dropwise between 0 and 30 min. A magnetic stirrer was used during online FTIR measurement.

Preparation of bituminous emulsion

Emulsifier product c (10 g) was dissolved in 200 mL water. The pH of the aqueous solution was adjusted to 2.0 by adding hydrochloric acid, and the solution was heated to 60 °C. AH-90 asphalt (300 g) was heated to 120 °C. The bituminous emulsion was prepared by mixing the aqueous solution containing emulsifier and asphalt in a colloid mill for 1 min.

Mixing experiment

Mineral aggregate (200 g) and 30 g water were placed in a 500-mL bowl. Bituminous emulsion (50 g) was then added, and the mixture was stirred at 60 revolutions per minute. The mixing time was recorded by observation of the mixing performance.

Results and discussion

Optimization to synthetic route to 2-(dodecyloxymethyl)oxirane

Univariate analysis was used to optimize the synthetic route to 2-(dodecyloxymethyl)oxirane. The factors feedstock mole ratio, reaction time, reaction temperature, and basicity were studied.

Feedstock mole ratio

The reaction conditions were: reaction temperature 50 °C, reaction time 5 h, basicity 33.3 %. Figure 1 shows a plot of the yield (Y) of product a versus feedstock mole ratio (m) of epichlorohydrin to lauryl alcohol. As shown in Fig. 1, the yield increases with increasing feedstock mole ratio then levels off for feedstock mole ratio greater than 1.4. Therefore, the optimum feedstock mole ratio is 1.4.

Reaction time

The reaction conditions were: reaction temperature 50 °C, feedstock mole ratio of epichlorohydrin to lauryl alcohol 1.4, basicity 33.3 %. Figure 2 shows a plot of yield versus reaction time (t). As shown in Fig. 2, the yield increases with

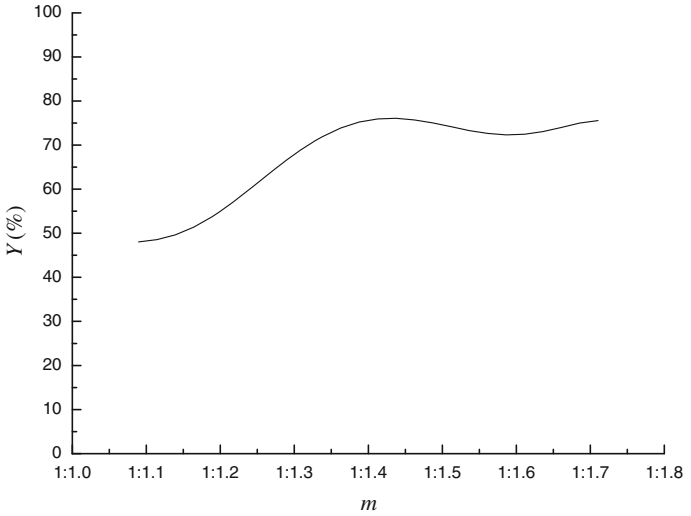

Fig. 1 Plot of yield versus feedstock mole ratio

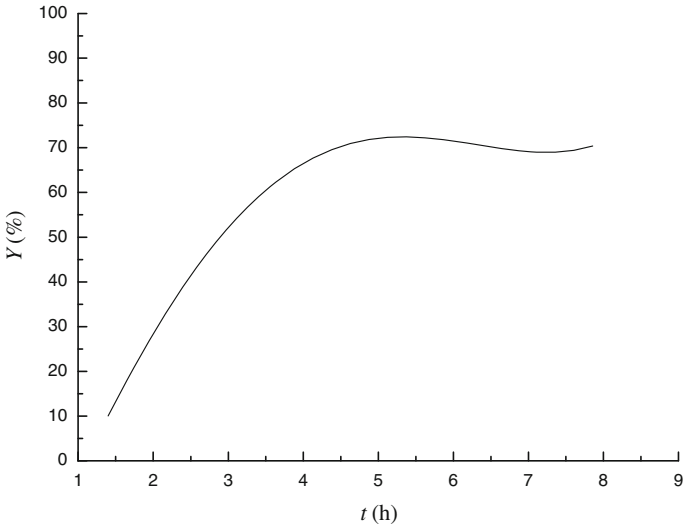

Fig. 2 Plot of reaction yield versus reaction time

increasing reaction time and levels off after 5 h. Therefore, the optimum reaction time is 5 h.

Reaction temperature

The reaction conditions were: reaction time 5 h, feedstock mole ratio of epichlorohydrin to lauryl alcohol 1.4, basicity 33.3 %. Figure 3 shows a plot of

yield versus reaction temperature (T). As shown in Fig. 3, the yield increases with increasing reaction temperature, and levels off after 50 °C. Therefore, the optimum reaction temperature is 50 °C.

Basicity

The reaction conditions were: reaction temperature 50 °C, reaction time 5 h, feedstock mole ratio of epichlorohydrin to lauryl alcohol 1.4. Figure 4 shows a plot of yield versus basicity (B). As shown in Fig. 4, the yield increases with increasing basicity, and levels off after 33.3 %. Therefore, the optimum basicity is 33.3 %.

Overall, the optimum reaction conditions were: reaction temperature 50 °C, reaction time 5 h, feedstock mole ratio of epichlorohydrin to lauryl alcohol 1.4, basicity 33.3 %. The yield reaches 75.7 % under the optimum conditions.

FTIR characterization

Figure 5 shows the FTIR spectrum of product a in Scheme 1. The absorption at 3,320 cm^{-1} (peak 1) is assigned to O–H stretching, which is attributed to ring opening of product a. The absorption at 3,049 cm^{-1} (peak 2) is assigned to C–H stretching in the epoxy group. The absorption near 2,926 cm^{-1} (peak 3) is assigned to methylene unsymmetrical stretching. The absorption near 2,853 cm^{-1} (peak 4) is assigned to methylene symmetrical stretching. The absorption at 1,465 cm^{-1} (peak 5) and 1,375 cm^{-1} (peak 6) is assigned to methylene unsymmetrical changing angle vibration. The absorption at 1,250 cm^{-1} (peak 7) originates from vibration of the

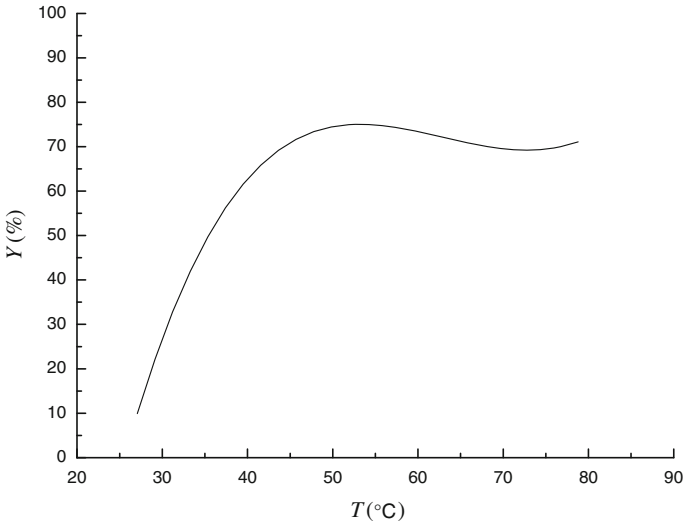

Fig. 3 Plot of reaction yield versus reaction temperature

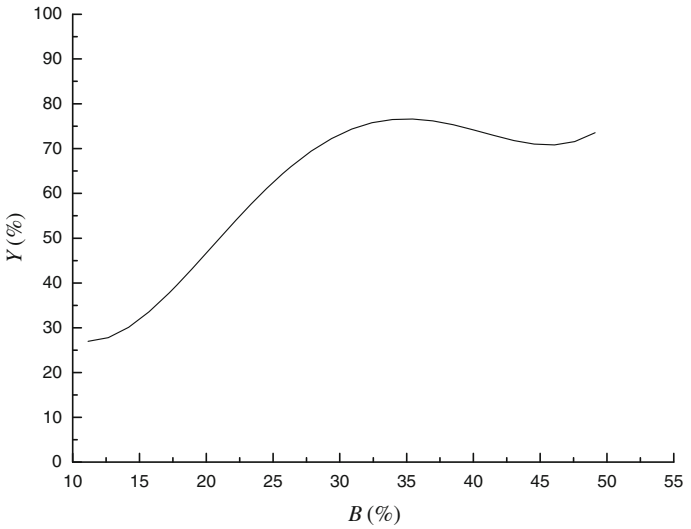

Fig. 4 The plot of reaction yield versus basicity

epoxy group. The absorption at 1,114 and 1,065 cm^{-1} (peak 8, 9) is assigned to asymmetrical and symmetrical stretching vibration, respectively, of C–O–C. The absorption at 950–810 cm^{-1} (peaks 10, 11) is assigned to the epoxy group. The absorption at 720 cm^{-1} (peak 12) is assigned to methylene in-plane swing vibration. Therefore, the FTIR spectrum agrees with the chemical structure of the target compound of the synthesis, product a.

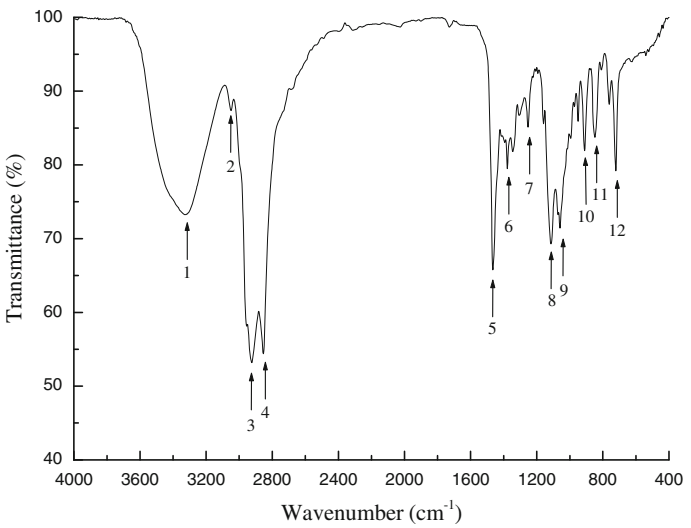

Fig. 5 FTIR spectrum of product a in Scheme 1

Figure 6 shows the FTIR spectrum of product b in Scheme 1. The broad absorption at 3,280–3,380 cm^{-1} (peak 1) is assigned to O–H stretching. The absorption at 2,926 and 2,853 cm^{-1} (peaks 2, 3) is assigned to asymmetrical and symmetrical stretching vibration, respectively, of methylene C–H. The absorption at 1,465 cm^{-1} (peak 4) and 1,385 cm^{-1} (peak 5) is assigned to methylene unsymmetrical changing angle vibration. The absorption at 1,336 cm^{-1} (peak 6) is attributed to in-plane deformation vibration of O–H. The absorption around 1,195 cm^{-1} (peak 7) is assigned to C–N stretching. The absorption at 1,125 and 1,065 cm^{-1} (peaks 8, 9) is assigned to asymmetrical and symmetrical stretching vibration, respectively, of C–O–C. The absorption at 722 cm^{-1} (peak 10) is assigned to methylene in-plane swing vibration. Therefore, the FTIR spectrum agrees with the chemical structure of the target compound of the synthesis, product b.

Figure 7 shows the FTIR spectrum of product c in Scheme 1. The broad band at 3,280–3,360 cm^{-1} (peak 1) is assigned to O–H stretching. The absorption near 2,926 cm^{-1} (peak 2) is assigned to methylene unsymmetrical stretching. The absorption near 2,853 cm^{-1} (peak 3) is assigned to methylene symmetrical stretching. The strong absorption at 1,740–1,760 cm^{-1} (peak 4) originates from C=O stretching in the carboxyl group. The absorption at 1,630–1,600 cm^{-1} (peak 5) is assigned to C=O stretching in carboxylate ($–COO^-$). The absorption at 1,465 cm^{-1} (peak 6) is assigned to methylene unsymmetrical changing angle vibration. The absorption at 1,414 cm^{-1} (peak 7) is attributed to the in-plane deformation vibration of O–H. The absorption at 1,180 cm^{-1} (peak 8) is assigned to C–N stretching. The absorption at 1,125 cm^{-1} (peak 9) is assigned to asymmetrical stretching vibration of C–O–C. The absorption at 720 cm^{-1} (peak 10) is assigned to the methylene in-plane swing vibration. Therefore, the FTIR spectrum agrees with the chemical structure of the target compound of the synthesis, product c.

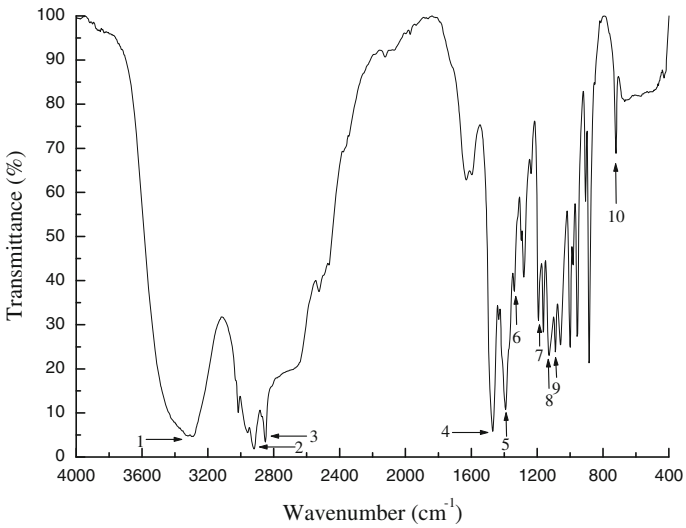

Fig. 6 FTIR spectrum of product b in Scheme 1

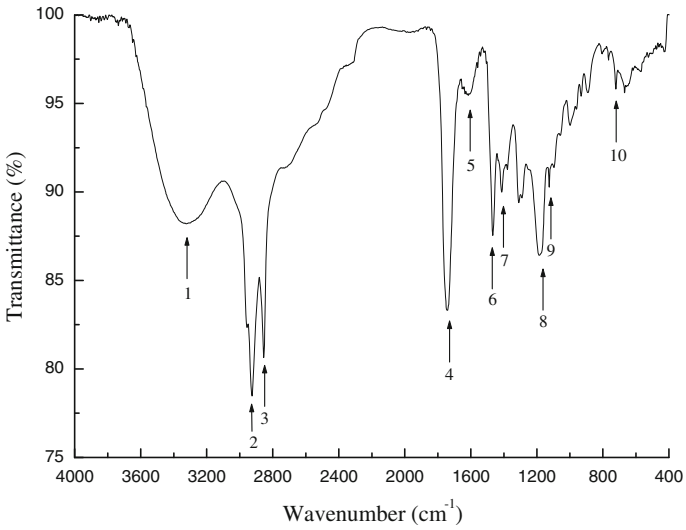

Fig. 7 FTIR spectrum of product c in Scheme 1

UV–visible spectroscopic characterization

Lauryl alcohol does not have absorption peak in the range of 200–1,000 nm. Product c has a strong absorption peak at 219 nm, which is attributed to the $n \rightarrow \pi^*$ band of the carboxy group in the molecule. The molar absorptivity (ε) of product c is 63.3 L mol^{-1} cm^{-1} in ethanol at 219 nm.

Online FTIR analysis

The reaction used to synthesize 2-(dodecyloxymethyl)oxirane was monitored by online FTIR. In the reaction, epichlorohydrin was added dropwise between 0 and 30 min and the reaction time was up to 6.5 h. Figure 8 shows the 3D online infrared spectrum throughout the whole reaction process. It is apparent the spectrum changed substantially. The most distinguishing change occurred after 40 min, which indicated the reaction speed increased substantially. Figure 9 shows the online infrared spectra at the beginning, middle, and end of the reaction, acquired at 0, 4.0, and 6.5 h, respectively.

Five components were detected automatically during the online FTIR analysis; their FTIR spectra are shown in Figs. 10, 11, 12, 13, and 14. In the FTIR spectrum of component 1 (Fig. 10), the absorption at 2,963 cm^{-1} (peak 1) is assigned to methyl unsymmetrical stretching. The absorption near 2,926 cm^{-1} (peak 2) is assigned to methylene unsymmetrical stretching. The absorption near 2,854 cm^{-1} (peak 3) is assigned to methylene symmetrical stretching. The absorption at 1,464 cm^{-1} (peak 4) and 1,376 cm^{-1} (peak 5) is assigned to methylene unsymmetrical changing angle vibration. The absorption at 1,252 cm^{-1} (peak 6) originates from vibration of the epoxy group. The absorption at 1,114 and 1,069 cm^{-1}

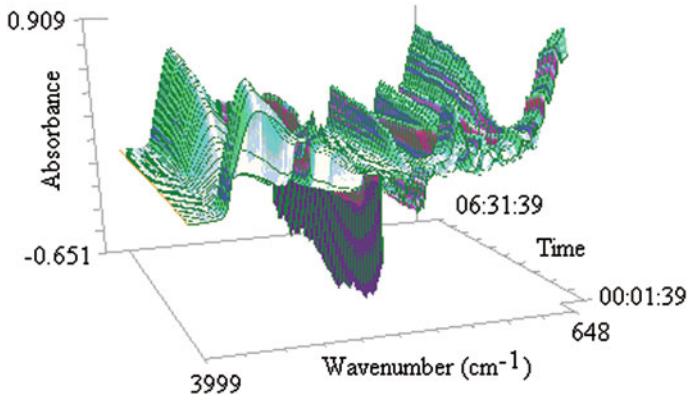

Fig. 8 3D online FTIR spectrum during the reaction

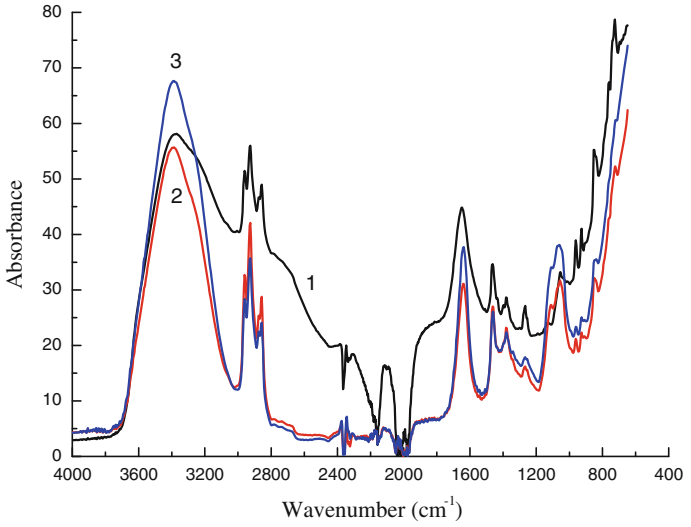

Fig. 9 Online infrared spectra at different stages of the reaction (*spectrum 1* at the beginning, *spectrum 2* in the middle, *spectrum 3* at the end)

(peaks 7, 8) is assigned to the asymmetrical and symmetrical stretching vibration, respectively, of C–O–C. The absorption at 950–810 cm^{-1} (peak 9) is assigned to the epoxy group. The absorption at 722 cm^{-1} (peak 10) is assigned to methylene in-plane swing vibration. Therefore, the spectrum of component 1 obtained by online FTIR agrees with the chemical structure of the target compound of the synthesis, product a.

In the FTIR spectrum of component 2 (Fig. 11), the absorption at 3,005 cm^{-1} (peak 1) is assigned to C–H stretching in the epoxy group. The absorption near 2,945 cm^{-1} (peak 2) is assigned to methylene unsymmetrical stretching. The absorption near 2,886 cm^{-1} (peak 3) is assigned to methylene symmetrical

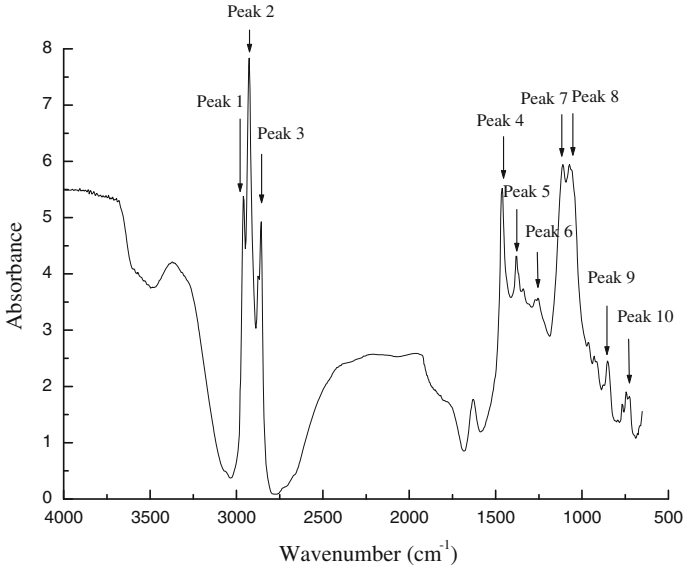

Fig. 10 The infrared spectrum of component 1 during the reaction

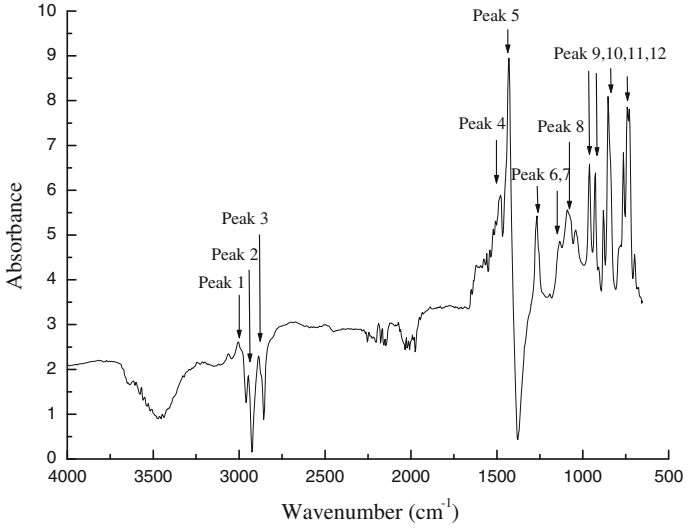

Fig. 11 The infrared spectrum of component 2 during the reaction

stretching. The absorption at 1,475 cm^{-1} (peak 4) and 1,430 cm^{-1} (peak 5) is assigned to methylene unsymmetrical changing angle vibration. The absorption at 1,265 cm^{-1} (peak 6) is assigned to vibration of the epoxy group. The absorption at 1,134 and 1,088 cm^{-1} (peak 7, 8) is assigned to asymmetrical and symmetrical stretching vibrations, respectively, of C–O–C. The absorption at 960–927 cm^{-1} (peak 9, 10) is assigned to the epoxy group. The absorption near 852 cm^{-1} (peak

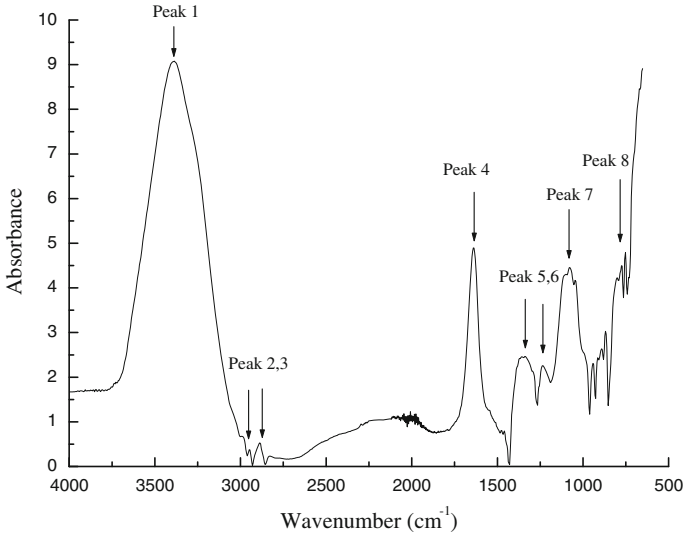

Fig. 12 The infrared spectrum of component 3 during the reaction

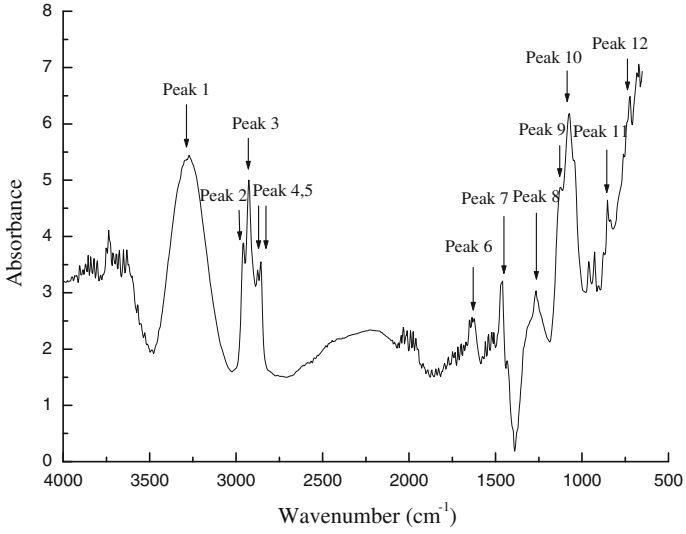

Fig. 13 The infrared spectrum of component 4 during the reaction

11) is assigned to C–Cl stretching. The absorption at 737–728 cm^{-1} (peak 12) is assigned to methylene in-plane swing vibration. Therefore, the spectrum of component 2 obtained by online FTIR could be that of the by-product shown in Scheme 2.

In the FTIR spectrum of component 3 (Fig. 12), the absorption at 3,389 cm^{-1} (peak 1) is assigned to O–H stretching. The absorption near 2,951 cm^{-1} (peak 2) is assigned to methylene unsymmetrical stretching. The absorption near 2,886 cm^{-1}

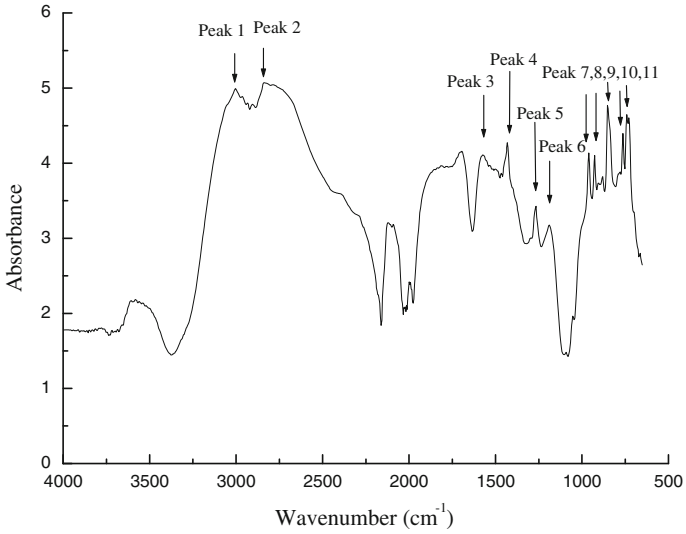

Fig. 14 The infrared spectrum of component 5 during the reaction

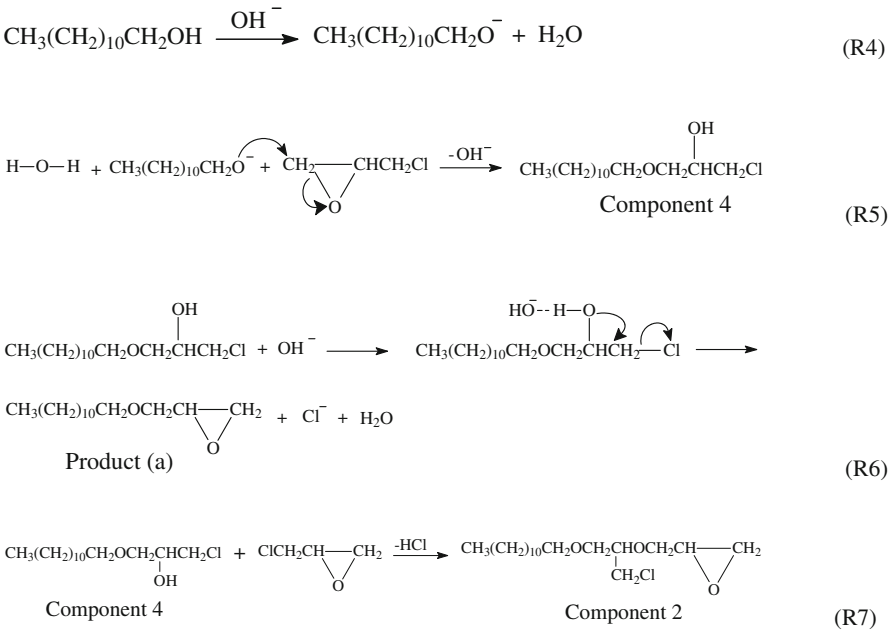

Scheme 2 The reaction mechanism for synthesis 2-(dodecyloxymethyl)oxirane

(peak 3) is assigned to methylene symmetrical stretching. The absorption at 1,460 cm^{-1} (peak 4) and 1,347 cm^{-1} (peak 5) is assigned to methylene unsymmetrical changing angle vibration. The absorption at 1,236 cm^{-1} (peak 6) originates from the deformation vibration of O–H. The absorption at 1,075 cm^{-1}

(peak 7) is assigned to C–O stretching. The absorption at 753 cm^{-1} (peak 8) is assigned to methylene in-plane swing vibration. Therefore, the spectrum of component 3 obtained by online FTIR agrees with the chemical structure of lauryl alcohol.

In the FTIR spectrum of component 4 (Fig. 13), the absorption at 3,260 cm^{-1} (peak 1) is assigned to O–H stretching. The absorption at 2,962 cm^{-1} (peak 2) is assigned to methyl unsymmetrical stretching. The absorption near 2,926 cm^{-1} (peak 3) is assigned to methylene unsymmetrical stretching. The absorption near 2,873 cm^{-1} (peak 4) is assigned to methyl symmetrical stretching. The absorption near 2,853 cm^{-1} (peak 5) is assigned to methylene symmetrical stretching. The absorption near 1,649 cm^{-1} (peak 6) is assigned to the O–H bending. The absorption at 1,465 cm^{-1} (peak 7) is assigned to methylene unsymmetrical changing angle vibration. The absorption at 1,265 cm^{-1} (peak 8) originates from the methylene out-of-plane swing vibration. The absorption at 1,125 cm^{-1} (peak 9) is assigned to asymmetrical stretching vibration of C–O–C. The absorption at 1,075 cm^{-1} (peak 10) is assigned to C–O stretching. The absorption near 855 cm^{-1} (peak 11) is assigned to C–Cl stretching. The absorption at 721 cm^{-1} (peak 12) is assigned to methylene in-plane swing vibration. Therefore, the spectrum of component 4 obtained by online FTIR could that of the intermediate shown in Scheme 2.

In the FTIR spectrum of component 5 (Fig. 14), the absorption at 3,002 cm^{-1} (peak 1) is assigned to C–H stretching in the epoxy group. The absorption near 2,829 cm^{-1} (peak 2) is assigned to methylene symmetrical stretching. The absorption at 1,570 cm^{-1} (peak 3) and 1,426 cm^{-1} (peak 4) is assigned to methylene unsymmetrical changing angle vibration. The absorption at 1,265 cm^{-1} (peak 5) originates from vibration of the epoxy group. The absorption at 1,190 cm^{-1} (peak 6) is assigned to asymmetrical stretching vibration of C–O–C. The absorption at 960–924 cm^{-1} (peaks 7, 8) is assigned to the epoxy group. The absorption near 848 cm^{-1} (peak 9) is assigned to C–Cl stretching. The absorption at 760–735 cm^{-1} (peaks 10, 11) is assigned to methylene in-plane swing vibration. Therefore, the spectrum of component 5 obtained by online FTIR could be that of epichlorohydrin.

Figure 15 shows the dependence of the relative concentrations (c) of components 1–5 on reaction time. As shown in Fig. 15, the relative concentration of component 1 increases sharply 40 min after epichlorohydrin was added, then remains constant. The relative concentration of component 1 decreases gradually with reaction time after 3 h, which is because of the side reaction shown in Scheme 2. Therefore, intermediate 1 could be the target compound of the synthesis, product a, in accordance with the changing trend of concentration and the online FTIR spectrum shown in Fig. 10.

The relative concentration of component 5 decreases sharply 40 min after epichlorohydrin was added, then decreases gradually with reaction time. Component 5 could be epichlorohydrin, in accordance with the changing trend of concentration and the online FTIR spectrum shown in Fig. 14.

The relative concentration of component 3 decreases sharply 40 min after epichlorohydrin was added, then keeps constant. Component 3 could be lauryl alcohol, in accordance with the changing trend of concentration and the online FTIR spectrum shown in Fig. 12.

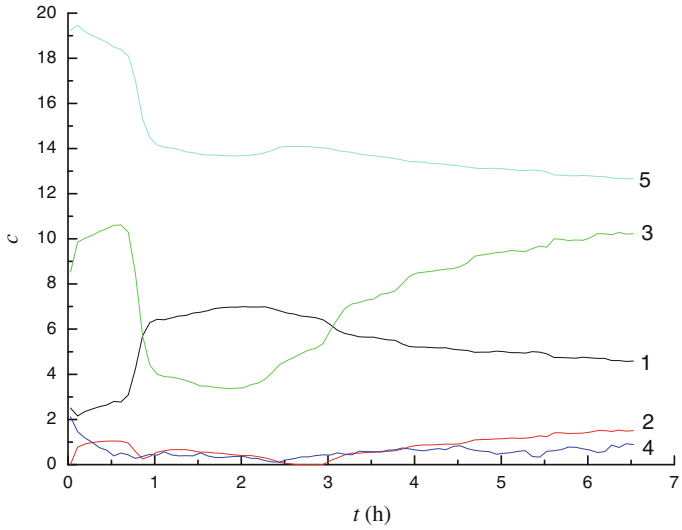

Fig. 15 Dependence on time of the relative concentrations of components 1–5

The relative concentration of component 4 decreases gradually with reaction time in the first stage, then keeps constant. Component 4 could be an intermediate, as shown in Scheme 2, in accordance with the changing trend of concentration and the online FTIR spectrum shown in Fig. 13.

The relative concentration of component 2 increases slightly with reaction time. Component 2 could be a by-product, as shown in Scheme 2, in accordance with the changing trend of concentration and the online FTIR spectrum shown in Fig. 11.

Reaction mechanism of synthesis 2-(dodecyloxymethyl)oxirane

For reaction R1 we proposed Scheme 2, as shown in reactions R4–R6, on the basis of the spectra obtained by online FTIR (Figs. 10, 11, 12, 13, 14) and the trends of the changing concentrations of the five components in Fig. 15. Component 4 is an intermediate in the synthesis 2-(dodecyloxymethyl)oxirane. As shown in reaction R4, lauryl alcohol is ionized in a highly basic environment. The alcohol anion is a strong nucleophile, and attacks the less substituted carbon atom of epichlorohydrin in an S_N2 reaction (reaction R5). The intermediate component 4 is formed. Cyclization of component 4 forms product a in reaction R6. Reaction R7 is a side reaction producing component 2 from component 4.

CMC and surface tension

Figure 16 shows the plot of surface tension (σ) versus the logarithm of the concentration of product c at 298 K. The surface tension decreased sharply at first then remained stable. The CMC has a lower value of 8.8×10^{-5} mol/L, which is located at the turning point of the curve. The surface tension at the CMC is 21.2 mN/m.

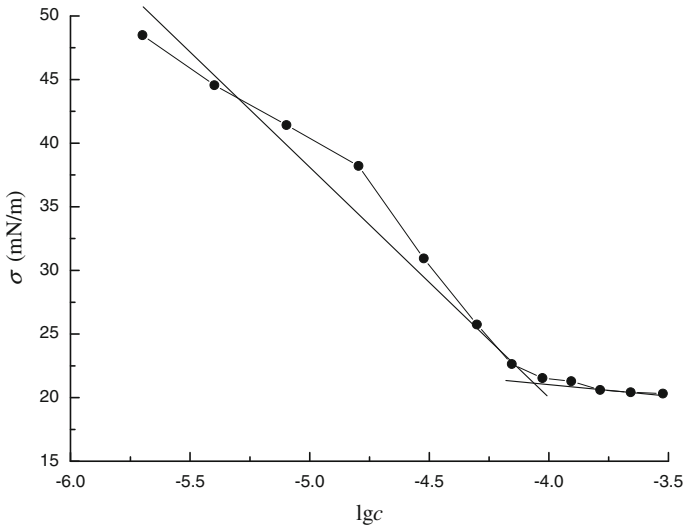

Fig. 16 Plot of surface tension against the logarithm of the concentration of product c

Mixing performance

The emulsifier c is an excellent emulsifier for asphalt. The prepared bituminous emulsion had higher storage stability. No separation of aqueous phase and asphalt phase occurred after 5 days. The mixing time was 30 s, which indicates the emulsifier is a rapid-set asphalt emulsifier. It can be designed to perform in a wide variety of applications including tack coat, fog seal, and solventless cold mix applications, for example recycling and base stabilization in asphalt pavement construction.

Conclusions

A novel betaine-type asphalt emulsifier was synthesized in three steps by reaction of lauryl alcohol, epichlorohydrin, dimethylamine, and chloroacetic acid. The optimum reaction conditions were obtained for the first step, synthesis of 2-(dodecyloxymethyl)oxirane. The intermediate was detected by use of online FTIR analysis during the first step of synthesis of 2-(dodecyloxymethyl)oxirane. On the basis of the experimental data, a plausible reaction mechanism was proposed for the reaction. The product has a low CMC, 8.8×10^{-5} mol/L. The surface tension at the CMC is 21.2 mN/m. The emulsifier of the product is a rapid-set asphalt emulsifier. It can be designed to perform in a wide variety of applications including tack coat, fog seal, and solventless cold mix applications, for example recycling and base stabilization in asphalt pavement construction.

References

1. H.I. Al-abdul Wahhab, I.M. Asi, Build. Environ. **32**, 271–279 (1997)
2. L.E. Chávez-valencia, E. Alonso, A. Manzano, J. Pérez, M.E. Contreras, C. Signoret, Constr. Build. Mater. **21**, 583–589 (2007)
3. Y. Niazi, M. Jalili, Constr. Build. Mater. **23**, 1338–1343 (2009)
4. H.H. Moorer, USP 4088505, 9 May 1978
5. W.T. Zdybak, USP 4427449, 24 Jan 1984
6. M.W. Shuey, R. S. Custer, USP 5650000, 15 Jul 1997
7. H.G. Schreuders, P. Schilling, USP 4447269, 5 May 1984
8. A. Jada, C. Florentin, S. Mariotti, Adv. Colloid Interface Sci. **108–109**, 127–132 (2004)
9. H. Shirai, Y. Tsushima, J. Sasaya, K. Komiya, JP 2001329176, 27 Nov 2001
10. P. Schilling, USP 6077888, 20 Jun 2000
11. G.G.I. Moore, M.S. Terrazas, USP 7164041, 16 Jan 2007
12. D.J. Tracy, R.X. Li, M.S. Dahanayake, J. Yang, USP 6204297. 20 Mar 2001
13. Y. Tomokzau, B. Miri, M. Keisuke, H. Chikako, E. Kazutoyo, J. Colloid Interface Sci. **339**, 230–235 (2009)
14. L. Shi, Z. Wan, L. Wang, Y. Xue, J. Shandong Univ (Eng Sc) **37**, 122–126 (2007)
15. P.E. Graf, S.J. Agazzi, E.J. Vanderzanden, USP 4985079, 15 Jan 1991
16. M. Velázquez M, F. Ortega, F. Monroy, R.G. Rubio, S. Pegiadou, L. Pérez, M.R. Infante, J. Colloid Interface Sci. **283**, 144–152 (2005)
17. J.L. Bigorra, N.B. Gilabert, M.O. Hernandez, X.C. Cruxens, R.P. Subirana, USP 6015780, 18 Jan 2000
18. J.M. Gonzalez, M.J. Bermejo, R.M. Barcelo, J. Vilaret, N. Siscart, USP 6683033, 27 Jan 2004
19. M. Chorro, N. Kamenka, B. Faucompre, M. Lindheimer, R. Zana, Colloids Surf A **110**, 249–261 (1996)
20. Y. Tomokazu, I. Tomoko, K. Megumi, E. Kunio, Colloids Surf A **273**, 208–212 (2006)
21. E.J. Pancheri, M.H.K. Mao, USP 5167872, 1 Dec 1992
22. M. Hellsten, I. Harwigsson, USP 5902784, 11 May 1999